THE JOURNAL OF PHYSICAL CHEMISTRY B

Article

pubs.acs.org/JPCB

Dansyl-Labeled Cholic Acid as a Tool To Build Speciation Diagrams for the Aggregation of Bile Acids

Miguel Gomez-Mendoza, M. Luisa Marin,* and Miguel A. Miranda*

Instituto Universitario Mixto de Tecnología Química (UPV-CSIC), Universitat Politècnica de València, Avenida de los Naranjos s/n, 46022 Valencia, Spain

Supporting Information

ABSTRACT: Bile acids (BAs) are a family of natural steroids biosynthesized from cholesterol in the liver that tend to form aggregates in solution. A fluorescent derivative of cholic acid, namely 3α-Dns-ChA, was employed as a reporter to establish the speciation diagrams of the most abundant BAs that can be found mainly in three microenvironments, solution, and primary and secondary aggregates. The developed methodology is based on the analysis of the combined steady-state and time-resolved experiments performed on 3α-Dns-ChA whose emission behavior was found to be strongly medium dependent. In particular, speciation diagrams of sodium glycocholate (NaGCh), sodium taurocholate (NaTCh), sodium chenodeoxycholate (NaCDCh), sodium glycochenodeoxycholate (NaGCDCh), sodium deoxycholate (NaDCh), and sodium ursodeoxycholate (NaUDCh) were successfully built up.

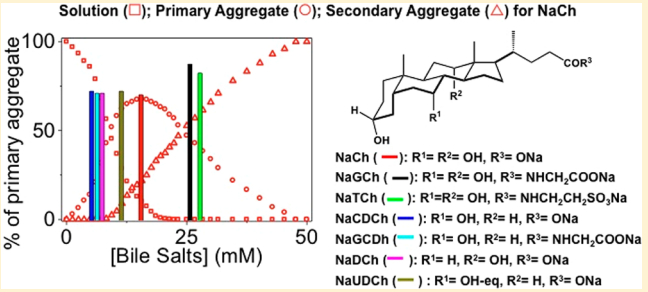

INTRODUCTION

Bile acids (BAs) are a family of natural steroids biosynthesized from cholesterol in the liver,[1] which play a key role in a number of physiological functions and are the major final products of cholesterol metabolism. Remarkably, they help lipid solubilization by forming mixed micelles and stimulate the biliary phospholipid secretion.[2,3]

The chemical structure of BAs includes an unusual cis fusion between rings A and B, a different number of hydroxyl groups on the α-face and a short chain ending in a carboxylic moiety. All these characteristics make them amphiphilic entities, with a hydrophilic α-face and a hydrophobic β-face, which results in a tendency to aggregate in solution. Natural BAs are divided into primary (cholic and chenodeoxycholic acid) directly biosynthesized from cholesterol and frequently found conjugated to glycine and taurine, and secondary (deoxycholic and lithocholic acids) obtained from the corresponding primary BAs after deconjugation of the amino acid and dehydroxylation at position C-7. Ursodeoxycholic acid is the C-7 epimer of chenodeoxycholic acid; it is found as a natural product in humans, at low concentrations, but it is used as an effective anticholestatic drug.[1,4−7] The structures of the corresponding bile salts (BSs) are shown in Chart 1.

The most widely accepted aggregation model postulates the formation of primary aggregates by interaction of the β-faces of few monomers (up to 10) at low BA concentrations, which agglomerate as the concentration increases, giving rise to secondary aggregates.[8] However, how the number of hydroxyl groups or the conjugation to glycine or taurine influences the aggregation behavior of the different BAs is not yet fully investigated. Moreover, the distribution of primary/secondary aggregates over a broad concentration range, needed to build the speciation diagram for every BA, has still to be addressed.

Chart 1. Chemical Structures of Primary and Secondary Bile Salts

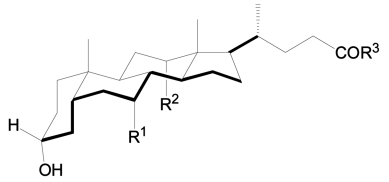

Sodium Cholate (**NaCh**): R^1= R^2= OH, R^3= ONa
Sodium Glycocholate (**NaGCh**): R^1= R^2= OH, R^3= $NHCH_2COONa$
Sodium Taurocholate (**NaTCh**): R^1= R^2= OH, R^3= $NHCH_2CH_2SO_3Na$
Sodium Chenodeoxycholate (**NaCDCh**): R^1= OH, R^2= H, R^3= ONa
Sodium Glycochenodeoxycholate (**NaGCDCh**): R^1= OH, R^2= H, R^3= $NHCH_2COONa$
Sodium Taurochenodeoxycholate (**NaTCDCh**): R^1= OH, R^2= H, R^3= $NHCH_2CH_2SO_3Na$
Sodium Deoxycholate (**NaDCh**): R^1= H, R^2= OH, R^3= ONa
Sodium Lithocholate (**NaLCh**): R^1= R^2= H, R^3= ONa
Sodium Ursodeoxycholate (**NaUDCh**): R^1= OH-eq, R^2= H, R^3= ONa

Several techniques have been employed to shed light on the aggregation behavior of BAs, including NMR[8,9] and photophysical techniques.[10−13] Specifically, pyrene has been used as a fluorescence probe to investigate the association of BSs in aqueous solution.[14−16] The ratio of the fluorescence intensities of the vibronic bands of pyrene is strongly dependent on solvent polarity, a property that has been exploited to

Received: August 30, 2012
Revised: October 21, 2012
Published: December 3, 2012

determine the critical micelle concentrations (cmcs).[17,18] Due to the fact that BS aggregates grow in size with increasing concentration, the cmc range of BSs is broader than that of other surfactants and hence difficult to be determined. Even more complex is the problem of estimating the relative amounts of BSs that can be found in the different aggregation stages. In a preliminary communication,[19] we have recently demonstrated that derivatization of cholic acid by incorporating a dansyl (Dns) fluorophore covalently attached to different positions of the skeleton (3α, 3β, or 7α)[20] gives rise to an appropriate medium-dependent fluorescent reporter on the aggregation behavior of sodium cholate, which can be successfully employed to build the speciation diagram of this bile salt. The concept is based on the enhancement of the emission quantum yields and lifetimes, upon incorporation into the aggregates. The unique properties of these ChA derivatives are associated with their close structural similarity to BSs, which allow them to occupy equivalent positions in the aggregates and results in a nearly negligible influence on micellization.

With this background, we wish now to report on the extension of this straightforward methodology to build speciation diagrams for sodium glycocholate (NaGCh), sodium taurocholate (NaTCh), sodium chenodeoxycholate (NaCDCh), sodium glycochenodeoxycholate (NaGCDCh), sodium deoxycholate (NaDCh), and sodium ursodeoxycholate (NaUDCh). For this purpose, the probe with a Dns unit bound to C-3α of cholic acid, namely 3α-Dns-ChA (Chart 2), has been selected as the fluorescent reporter.

Chart 2. Chemical Structure of 3α-Dns-ChA

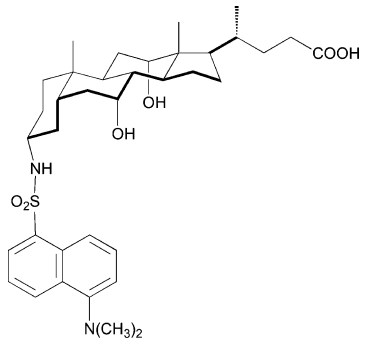

EXPERIMENTAL METHODS

Chemicals. The BA salts NaCh, NaGCh, NaTCh, NaCDCh, NaGCDCh, and NaDCh as well as lithocholic acid (LChA), ursodeoxycholic acid (UDChA), sodium chloride, sodium hydrogen carbonate, and dimethyl sulfoxide (DMSO), were purchased from Sigma Aldrich and used without further purification. The free acids LChA and UDChA were basified with the stoichiometric amount of $NaHCO_3$ to obtain the corresponding salts NaLCh and NaUDCh. Millipore water was used for sample preparation. The fluorescent reporter 3α-Dns-ChA was synthesized as previously described.[20]

Instrumentation. Absorption spectra were registered on a Cary 300 UV−vis spectrophotometer (UV0811M209, Varian). Fluorescence spectra were recorded with a LP S-220B (Photon Technology International) equipped with a 75 W Xe lamp. All the spectra were corrected with baseline control experiments to subtract the solvent Raman emission. Fluorescence lifetime measurements were obtained on a PTI (TM-2/2003) equipped with H_2/N_2 lamp (50/50, 1.5 ns pulse width) and a stroboscopic detector. The concentration of 3α-Dns-ChA (20 μM) ensured that the absorbance of all solutions was below 0.1 at the isosbestic point used in each case as the excitation wavelength (λ_{exc} = 327−360 nm for steady-state and λ_{exc} = 337 nm for time-resolved experiments, respectively). All the photophysical measurements were performed under air, at room temperature, in a quartz cell of 1.0 cm optical path length.

RESULTS AND DISCUSSION

In order to check the applicability of the methodology, the UV−vis spectrum of 3α-Dns-ChA (20 μM) was recorded in the presence of increasing concentrations of bile salts; this produced no noticeable effect on the long-wavelength absorption band (see Figure 1a for the case of NaGCh).

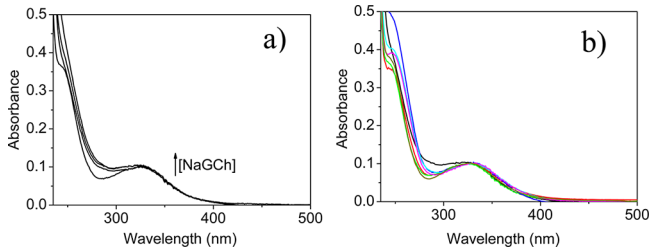

Figure 1. Absorption spectra of 3α-Dns-ChA (20 μM) (a) upon addition of increasing concentrations of NaGCh (0−100 mM), and (b) in the presence of 30 mM NaCh (red), NaGCh (black), NaTCh (green), NaCDCh (blue), NaGCDCh (turquoise), NaDCh (pink), and NaUDCh (brown), in 0.2 M aqueous NaCl.

Likewise, addition of 30 mM NaCh, NaGCh, NaTCh, NaCDCh, and NaUDCh did not have any influence on the absorption spectrum of the probe in the 325−360 nm region (see Figure 1b). Therefore, the excitation wavelength for the subsequent emission experiments was selected in this region. In the case of NaGCDCh and NaDCh, slight changes in the absorption spectra were noticed; this made steady-state emission measurements less reliable, but did not influence the time-resolved results, which allowed us to build the speciation diagrams. Unfortunately, the very scarce solubility of NaLCh in aqueous medium prevented the performance of photophysical experiments, and thus no further studies were carried out on this BS.

Then, 3α-Dns-ChA was subjected to steady-state emission measurements in the presence of increasing concentrations of NaCh, NaGCh, NaTCh, NaCDCh, and NaUDCh (see Figure 2a for the case of NaGCh). In general, addition of the BSs resulted in a marked enhancement of the emission intensities (Figure 2b), accompanied by a significant hypsochromic shift of the maximum (Figure 2c), as a result of the progressive incorporation of the fluorophore to the hydrophobic micro-environment provided by the BSs.

Furthermore, time-resolved measurements were performed for NaCh, NaGCh, NaTCh, NaCDCh, and UDCh, as well as for NaGCDCh and NaDCh. Thus, the lifetime of 3α-Dns-ChA was determined upon addition of increasing concentrations of BS. The fluorescence decays of 3α-Dns-ChA in the presence of NaGCh are shown in Figure 3a as an example.

In all cases, a significant increase of the average lifetime was observed as the concentration of BS increased (Figure 3b). It was also found that, at moderate BS concentrations, in addition to the known lifetime in aqueous solution (4.8 ns),[20] a second

dx.doi.org/10.1021/jp308624h | J. Phys. Chem. B 2012, 116, 14776−14780

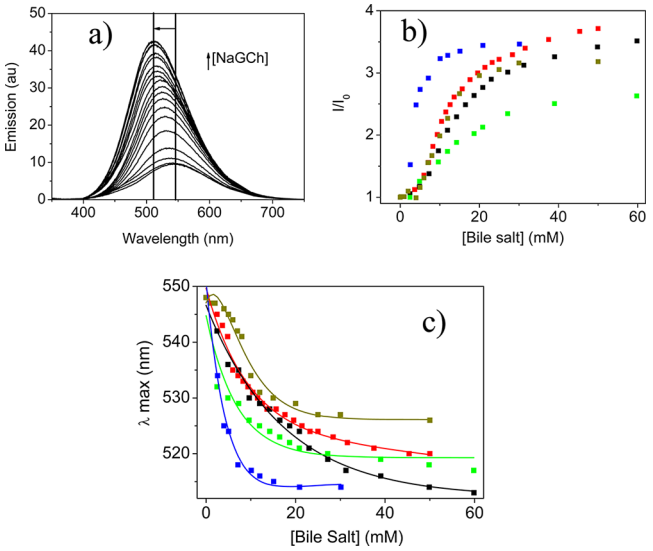

Figure 2. (a) Emission spectra of 3α-Dns-ChA (20 μM) in 0.2 M NaCl upon addition of increasing concentrations of NaGCh (λ_{exc} = 327 nm) in the range 0−100 mM. (b) Changes in the relative emission intensities (I/I_0). (c) Changes in the emission λ_{max} vs BS concentration for NaCh (red), NaGCh (black), NaTCh (green), NaCDCh (blue), and NaUDCh (brown) in 0.2 M aqueous NaCl.

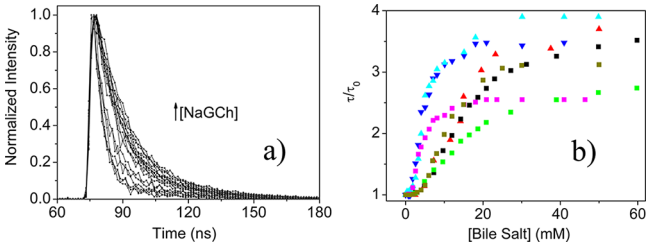

Figure 3. (a) Time-resolved fluorescence of 3α-Dns-ChA (20 μM) in 0.2 M aqueous NaCl upon addition of increasing concentrations of NaGCh (λ_{exc} = 337 nm). (b) Changes in the relative lifetime (τ/τ_0) vs BA concentration for NaCh (red), NaGCh (black), NaTCh (green), NaCDCh (blue), NaGCDCh (turquoise), NaDCh (pink), and NaUDCh (brown) in 0.2 M aqueous NaCl.

lifetime value (τ_I) had to be introduced to get a good fitting, which was taken as an indication of the formation of the primary aggregates. Moreover, at higher BS concentrations, a third lifetime (τ_{II}) was needed for a satisfactory fitting, in agreement with formation of the secondary aggregates. Table 1 shows the values found for the lifetimes of 3α-Dns-ChA (τ_I and τ_{II}) when incorporated into every studied BS. According to these data, incorporation of the probe into the primary aggregates provokes an increase of its fluorescence lifetime

Table 1. Fluorescence Lifetimes of 3α-Dns-ChA in Primary (I) and Secondary (II) Aggregates

	τ_I (ns)	τ_{II} (ns)
NaCh	10.6	12.8
NaGCh	12.1	16.5
NaTCh	11.6	13.2
NaCDCh	8.5	15.5
NaGCDCh	9.5	17.2
NaDCh	9.5	12.3
NaUDCh	9.0	14.9

that is more than twice the value found in solution. Formation of the secondary aggregates is also associated with a lifetime enhancement, which is especially remarkable in the case of NaCDCh and its conjugate derivative NaGCDCh.

Interestingly, when the changes in the relative fluorescence intensities (I/I_0) or in the average lifetimes (τ/τ_0) of 3α-Dns-ChA versus BS concentration were plotted together (see Figure 4 for NaGCh), it became evident that the two methodologies reveal exactly the same trend, which can be taken as a proof for the dynamic nature of the observed emission changes.

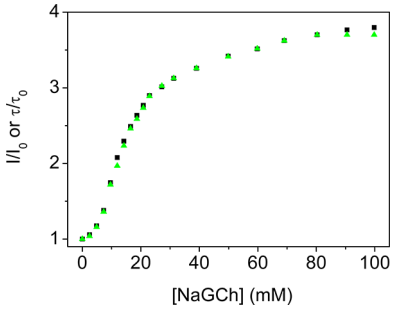

Figure 4. Changes in the relative emission intensities (I/I_0) (black squares) or lifetimes (τ/τ_0) (green triangles) vs NaGCh concentration in 0.2 M aqueous NaCl.

After the emission behavior of 3α-Dns-ChA as a function of added BS concentration was examined, a further effort was made to build the speciation diagrams for all BAs. For this purpose, the percentage of each component in 0.2 M aqueous NaCl (% i) within the different microenvironments, i.e., solution (% S), primary aggregates (% I), and secondary aggregates (% II), was determined using eqs 1 and 2.

$$\frac{I}{I_0} = \frac{(\%S)\phi_S + (\%I)\phi_I + (\%II)\phi_{II}}{100\phi_S} \quad (1)$$

$$\%i = \frac{100\frac{A_i}{\phi_i}}{\frac{A_S}{\phi_S} + \frac{A_I}{\phi_I} + \frac{A_{II}}{\phi_{II}}} \quad (2)$$

where I/I_0 is the emission enhancement at a given BS concentration, ϕ_S, ϕ_I, and ϕ_{II} are the corresponding fluorescence quantum yields, and A_S, A_I, and A_{II} are the pre-exponential factors of the decay fittings in the time-resolved experiments.

The value of ϕ_S determined for 3α-Dns-ChA was 0.05; the values of ϕ_{II} were initially estimated assuming that, when the plateau is reached, at high BS concentration, secondary aggregates are the overwhelmingly predominating species. Primary aggregates are expected to predominate in the intermediate BA concentration range. Therefore, initial ϕ_I values were selected by assuming the simplification that primary aggregates are the only existing species at intermediate concentration. In the case of NaGCDCh and NaDCh, for which the steady-state experiments were less reliable, the values of ϕ_I and ϕ_{II} were taken from the plot of the relative lifetimes versus BS concentration. This is based on the parallelism between the steady-state and the time-resolved behaviors, which was already demonstrated for the other BAs (see Figure 4). The first estimated quantum yield values were fed into eqs 1 and 2 and subsequently refined within ±0.02 until the

dx.doi.org/10.1021/jp308624h | J. Phys. Chem. B 2012, 116, 14776−14780

simulated results were superimposable to the experimental ones. The final quantum yield values are shown in Table 2.

Table 2. Fluorescence Quantum Yields of 3α-Dns-ChA in Primary (I) and Secondary (II) Aggregates Determined by Applying Eqs 1 and 2

	ϕ_I[a]	ϕ_{II}[a]
NaCh	0.14	0.19
NaGCh	0.13	0.19
NaTCh	0.12	0.14
NaCDCh	0.13	0.18
NaGCDCh	0.13	0.20
NaDCh	0.11	0.18
NaUDCh	0.10	0.16

[a]Errors were lower than 5% of the stated values.

With the determined percentage of each species (% *i*) it was possible to build the speciation diagrams of each BA as shown in Figure 5. Significant differences can be found among the seven studied analogues. For instance, in the case of NaCh and the corresponding glycine and taurine derivatives (Figure 5a–c), it is clear that conjugation results in more hydrophilic BAs that extend their presence in solution until 40 mM. In accordance with this increased solubility, the maximum concentration for the primary aggregates is reached at 25–30 mM while for NaCh it is reached at ca. 15 mM (see Figure 6).

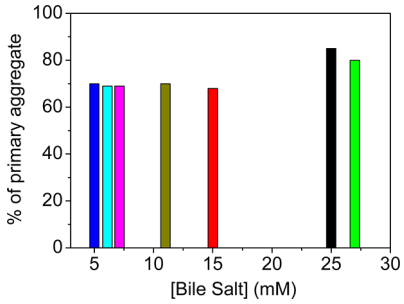

Figure 6. Composition between the BA concentrations where the percentage of primary aggregates is maximized for NaCh (red), NaGCh (black), NaTCh (green), NaCDCh (blue), NaGCDCh (turquoise), NaDCh (pink), and NaUDCh (brown) in 0.2 M aqueous NaCl.

In addition, the lack of a hydroxyl group at position C-12 has also a marked influence on the distribution of the three species, as shown for NaCDCh and NaGCDCh (Figure 5d,e). Their presence in the bulk solution is scarce above 8 mM, and the primary aggregates are predominating at around 5 mM (Figure 6). Again, the increased solubility due to conjugation with the

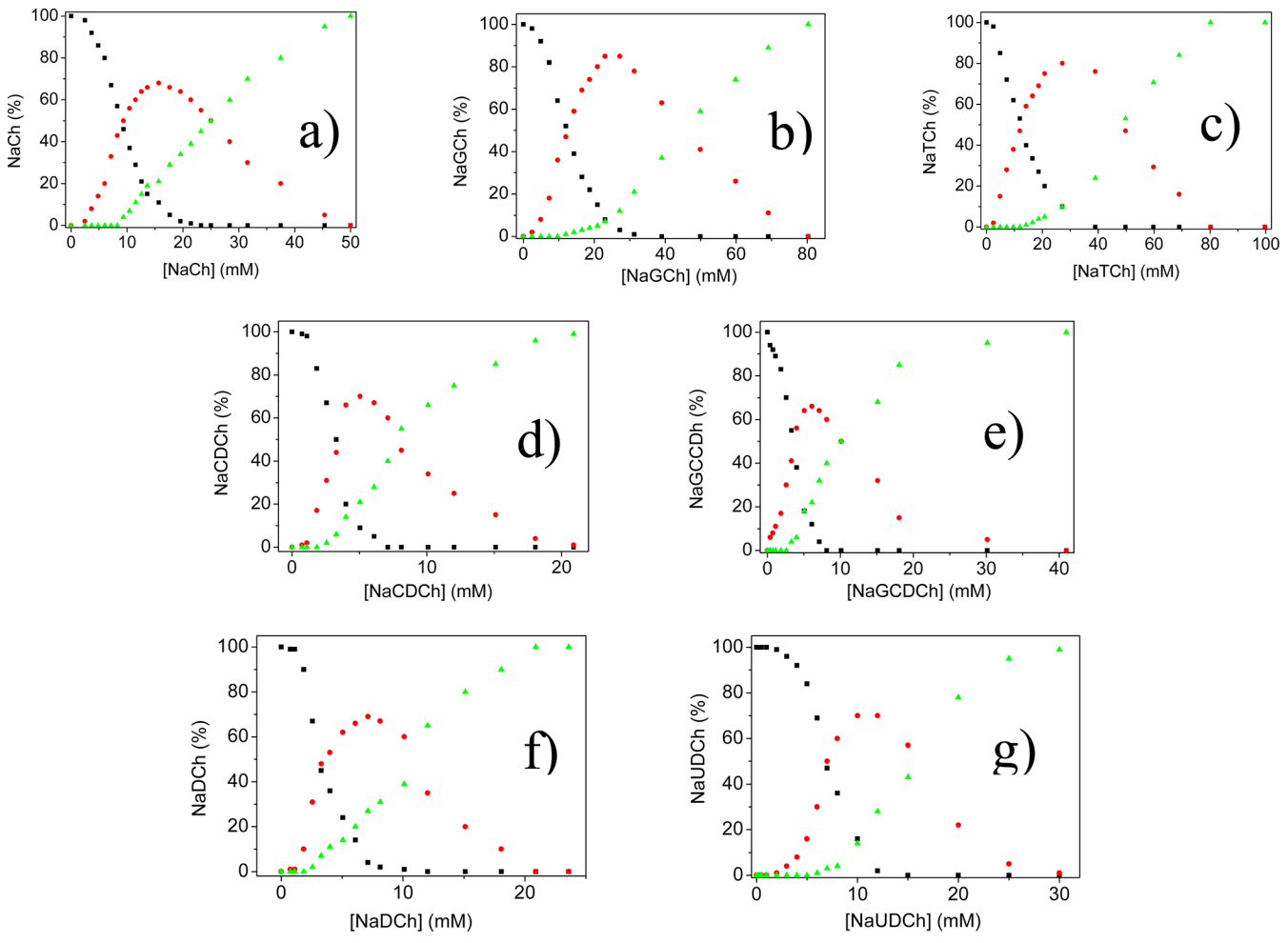

Figure 5. Percentage of BA in solution (black squares), in primary (red circles) and secondary aggregates (green triangles) for (a) NaCh; (b) NaGCh; (c) NaTCh; (d) NaCDCh; (e) NaGCDCh; (f) NaDCh; and (g) NaUDCh.

dx.doi.org/10.1021/jp308624h | J. Phys. Chem. B 2012, 116, 14776–14780

amino acid moves the three curves to higher concentrations, although in this case the effect is less remarkable than in the NaCh/NaGCh pair. As expected, very similar speciation diagrams were found for NaCDCh (Figure 5d) and NaDCh (Figure 5f), since both contain two hydroxyl groups in the α-face; changing the hydroxyl group at C-7 to the β-face of the skeleton as in NaUDCh results in a higher solubility (Figure 5g), and therefore the maximum percentages of primary aggregates appear at higher concentration (Figure 6). This is interesting in connection with the pharmacological activity of NaUDCh, which has been attributed in part to the fact that its administration to patients renders the BA composition of bile less hydrophobic, reducing the concentration of NaCDCh/NaGCDCh and NaDCh/NaGDCh and hence the toxic potential.[21,22] Overall, the observed trends are in reasonable agreement with the cmc values determined by independent methods, such as that based on the relative intensities of the vibronic bands in the pyrene fluorescence spectrum.[16] However, speciation diagrams are much more informative than just cmcs, and the fact that a single Dns-labeled BA can be used to probe aggregation in a full series of analogues constitutes a general validation of the methodology.

CONCLUSIONS

In summary, the usefulness of 3α-Dns-ChA as a fluorescent reporter to establish the distribution of the most abundant bile acids in the main three microenvironments, solution, and primary and secondary aggregates, has been demonstrated. The developed methodology is based on the combined analysis of steady-state and time-resolved experiments, which reveal a strongly medium-dependent emission behavior. The obtained information can be advantageously used to build the speciation diagrams, where clear differences associated with the degree of hydroxylation and/or conjugation have been found.

ASSOCIATED CONTENT

Supporting Information

Absorption spectra, steady-state spectra, time-resolved decays, and comparison of experiments of the bile acids. This material is available free of charge via the Internet at http://pubs.acs.org.

AUTHOR INFORMATION

Corresponding Author

*E-mail: marmarin@qim.upv.es (M.L.M.); mmiranda@qim.upv.es (M.A.M.). Fax: +34963879444. Tel: +34963877807.

Notes

The authors declare no competing financial interest.

ACKNOWLEDGMENTS

We gratefully acknowledge financial support from the Generalitat Valenciana (GV/2009/104 and Prometeo 2008/090), the Spanish Government (Red RETICS de Investigación de Reacciones Adversas a Alergenos y Fármacos (RIRAAF), CTQ2009-13699, and Predoctoral FPU fellowship AP2008-03295 for M.G.-M.).

REFERENCES

(1) Hofmann, A. F.; Mysels, K. J. *Colloids Surf.* **1988**, *30*, 145−173.
(2) Hofmann, A. F. *Arch. Intern. Med.* **1999**, *159*, 2647−2658.
(3) Hofmann, A. F.; Hagey, L. R. *Cell. Mol. Life Sci.* **2008**, *65*, 2461−2483.
(4) Armstrong, M. J.; Carey, M. C. *J. Lipid Res.* **1982**, *23*, 70−80.
(5) Hofmann, A. F. *Am. J. Surg.* **1989**, *158*, 198−204.
(6) Crosignani, A.; Battezzati, P. M.; Setchell, K. D. R.; Invernizzi, P.; Covini, G.; Zuin, M.; Podda, M. *Dig. Dis. Sci.* **1996**, *41*, 809−815.
(7) Crosignani, A.; Setchell, K. D. R.; Invernizzi, P.; Larghi, A.; Rodrigues, C. M. P.; Podda, M. *Clin. Pharmacokinet.* **1996**, *30*, 333−358.
(8) Small, D. M.; Penkett, S. A.; Chapman, D. *Biochim. Biophys. Acta* **1969**, *176*, 178−189.
(9) Paul, R.; Mathew, M. K.; Narayanan, R.; Balaram, P. *Chem. Phys. Lipids* **1979**, *25*, 345−356.
(10) Ju, C.; Bohne, C. *Photochem. Photobiol.* **1996**, *63*, 60−67.
(11) Rinco, O.; Nolet, M. C.; Ovans, R.; Bohne, C. *Photochem. Photobiol. Sci.* **2003**, *2*, 1140−1151.
(12) Li, R.; Carpentier, E.; Newell, E. D.; Olague, L. M.; Heafey, E.; Yihwa, C.; Bohne, C. *Langmuir* **2009**, *25*, 13800−13808.
(13) Diaz, A. N.; Sanchez, F. G.; Pareja, A. G. *Colloids Surf. A−Physicochem. Eng. Asp.* **1998**, *142*, 27−34.
(14) Zana, R.; Guveli, D. *J. Phys. Chem.* **1985**, *89*, 1687−1690.
(15) Matsuoka, K.; Maeda, M.; Moroi, Y. *Colloids Surf. B−Biointerfaces* **2003**, *32*, 87−95.
(16) Ninomiya, R.; Matsuoka, K.; Moroi, Y. *Biochim. Biophys. Acta* **2003**, *1634*, 116−125.
(17) Kalyanasundaram, K.; Thomas, J. K. *J. Am. Chem. Soc.* **1977**, *99*, 2039−2044.
(18) López-Díaz, D.; Velázquez, M. M. *Chem. Educ.* **2007**, *12*, 327−330.
(19) Gomez-Mendoza, M.; Marin, M. L.; Miranda, M. A. *J. Phys. Chem. Lett.* **2011**, *2*, 782−785.
(20) Rohacova, J.; Marin, M. L.; Martinez-Romero, A.; O'Connor, J. E.; Gomez-Lechon, M. J.; Donato, M. T.; Castell, J. V.; Miranda, M. A. *Org. Biomol. Chem.* **2009**, *7*, 4973−4980.
(21) Paumgartner, G.; Beuers, U. *Clin. Liver Dis.* **2004**, *8*, 67−81.
(22) Moroi, Y.; Okabe, M. *Colloids Surf. A−Physicochem. Eng. Asp.* **2000**, *169*, 75−84.